Biochimica et Biophysica Acta 1808 (2011) 1811–1817

Contents lists available at ScienceDirect

Biochimica et Biophysica Acta

journal homepage: www.elsevier.com/locate/bbamem

A mechanistic investigation of cell-penetrating Tat peptides with supported lipid membranes

Stefania Piantavigna [a], George A. McCubbin [a], Solveig Boehnke [a], Bim Graham [b], Leone Spiccia [a], Lisandra L. Martin [a,*]

[a] School of Chemistry, Monash University, Clayton, Victoria 3800, Australia
[b] Medicinal Chemistry and Drug Action, Monash Institute of Pharmaceutical Sciences, Monash University, Parkville, Victoria 3052, Australia

ARTICLE INFO

Article history:
Received 20 December 2010
Received in revised form 8 March 2011
Accepted 9 March 2011
Available online 15 March 2011

Keywords:
Tat peptide
Quartz crystal microbalance
Disruption
Antimicrobial peptide
Peptide antibiotic

ABSTRACT

The multifarious Tat peptide derived from the HIV-1 virus exhibits antimicrobial activity. In this article, we use Quartz Crystal Microbalance with Dissipation monitoring (QCM-D) to investigate the mechanisms of action of Tat (44–57) and Tat (49–57) on bacterial-mimetic 1,2-dimyristoyl-*sn*-glycero-3-phosphocholine (DMPC)/1,2-dimyristoyl-*sn*-glycero-3-phospho-*rac*-(1-glycerol) (sodium salt) (DMPG) membranes. The results reveal that both peptides disrupt DMPC/DMPG membranes via a surface-active (carpet-like) mechanism. The magnitude of this disruption is dependent on both membrane and peptide properties. Firstly, less disruption was observed on the more negatively charged membranes. Secondly, less disruption was observed for the longer and slightly more hydrophobic Tat (44–57) peptide. As a comparison, the behaviour of the two Tat peptides on mammalian-mimetic DMPC/cholesterol membranes was investigated. Consistent with the literature no membrane disruption was observed. These results suggest that both electrostatic and hydrophobic interactions, as well as peptide geometry, determine the antimicrobial activity of Tat. This should guide the development of more potent Tat antibiotics.

1. Introduction

The increasing number of antibiotic-resistant bacteria and the decreasing number of new antibiotics in development are leading to a public health crisis [1,2]. Antimicrobial peptides (AMPs) are a promising solution because they are generally selective for bacterial membranes; they have broad-spectrum antibacterial activity and some show antifungal, antiviral and anticancer activity; and the development of bacterial resistance to AMPs is difficult [3–8]. AMPs are also a realistic solution with, for example, MSI-78 (Pexiganan) reaching phase III clinical trials for topical treatment of diabetic foot ulcers (although FDA approval was later denied) [9]. Recently, it was demonstrated by Jung and co-workers that the HIV-1 virus nuclear transcription activating protein Tat (residues 47–58) exhibits anti-fungal and antibacterial activity [10,11]. Importantly, Tat (47–58) exerted toxic activity towards all multi-drug resistant *Staphylococcus aureus* and *Pseudomonas aeruginosa* strains tested (with minimum inhibitory concentrations (MICs) of 0.625–20 μM), had no hemolytic activity over that range, and the D-enantiomer was resistant to proteolytic degradation, making it a potential therapeutic agent [11].

In contrast to the hotly debated mechanism of action of Tat on eukaryotic cells [12–14], there are relatively few studies concerning how Tat exerts its antibacterial activity. The current view is that, firstly, on addition of Tat to bacterial-mimetic liposomes consisting of phosphocholine (PC) and phosphoglycerol (PG) lipids, Tat binds with high affinity and remains unstructured on the membrane surface [15,16]. The binding of the positively charged Tat to the negatively charged PC/PG membrane results in charge neutralisation, which facilitates liposome aggregation [17]. Fusion was then observed for the unsaturated dioleoyl (DO) liposomes, which suggests that binding causes membrane destabilisation [17]. However, any Tat-induced membrane destabilisation is small, as fluorescent dye leakage experiments showed that only <10% of the entrapped dye was released from the PC/PG liposomes [15,17]. Furthermore, Tat caused negligible membrane depolarisation of *Staphylococcus aureus* cells [18]. These results suggest that Tat does not act via a pore or carpet mechanism [19]. Instead, it is thought that Tat translocates through bacterial membranes and acts on an intracellular target [18], as observed for its antifungal activity [10] and for other AMPs [20,21]. While Tat is non-disruptive, dimerisation of the peptide at the C-terminus confers a membrane-disruptive mode of action [18].

Quartz Crystal Microbalance with Dissipation monitoring (QCM-D) has been employed by us and others to investigate the mode of action of AMPs [20–26]. A biomimetic lipid membrane can be deposited onto the QCM-D sensor 'chips' in situ [27]. Upon addition of an AMP solution, the mass and structural changes to the lipid membrane can be monitored in real time by the QCM-D instrument. QCM-D can therefore provide direct information about the effect of the AMP on

* Corresponding author. Tel.: +61 3 99054514; fax: +61 3 99054597.
E-mail address: Lisa.Martin@monash.edu (L.L. Martin).

0005-2736/$ – see front matter © 2011 Elsevier B.V. All rights reserved.
doi:10.1016/j.bbamem.2011.03.002

the lipid membrane, without the need for dyes or other chemicals. In this study, QCM-D is used to investigate the behaviour of Tat (44–57) (Ac-GISYGRKKRRQRRR-NH_2, basic residues are underlined) and Tat (49–57) (Ac-RKKRRQRRR-NH_2) on bacterial-mimetic membranes and, as a comparison, mammalian-mimetic membranes. Consistent with the reported non-lytic activity of Tat on eukaryotic cells, we show that both Tat peptides add to the membrane with no loss of mass. However, in contrast to the current literature, Tat is shown to disrupt bacterial membranes via a surface-active mechanism. Reasons for this discrepancy are considered.

2. Materials and methods

2.1. Peptide synthesis

Tat (44–57) and Tat (49–57) with N-terminal acetylation and C-terminal amidation were synthesised with L-amino acids by automated solid phase peptide synthesis on a Rink amide resin.

2.2. Buffer preparation

Sodium chloride (≥99.5%), potassium phosphate monobasic (anhydrous, ≥99.0%) and potassium phosphate dibasic (anhydrous, ≥98%) were purchased from Sigma-Aldrich (Castle Hill, Australia). Ultrapure water was used with an initial resistivity of 18.2 MΩ·cm (Sartorius AG, Göttingen, Germany). Phosphate buffered saline (PBS, pH 6.9 ± 0.1) was prepared having 20 mM phosphate and either 100 mM ("high-salt") or 30 mM ("low-salt") sodium chloride in water.

2.3. Liposome preparation

1,2-Dimyristoyl-*sn*-glycero-3-phosphocholine (DMPC) and 1,2-dimyristoyl-*sn*-glycero-3-phospho-*rac*-(1-glycerol) (sodium salt) (DMPG) were purchased from Avanti Polar Lipids (Alabaster, USA). Cholesterol, chloroform (≥99.8%) and methanol (≥99.9%) were purchased from Sigma-Aldrich (Castle Hill, Australia). DMPC and cholesterol were dissolved in chloroform and DMPG was dissolved in chloroform/methanol (ca. 3:1) to create individual 5 mM stock solutions. These solutions were then aliquoted into test tubes to obtain the desired lipid composition (DMPC/cholesterol 7:3 v/v, and DMPC/DMPG 4:1 and 2:1 v/v). The solvent was evaporated under N_2 and the test tubes were then dried under vacuum. To prepare the liposomes, the lipids were resuspended in high-salt PBS (100 mM NaCl) to a lipid concentration of 0.5 mM and then incubated at 37 °C, vortexed and briefly sonicated (<5 min) in a bath sonicator before use. The resultant liposomes are unilamellar and have a bimodal size distribution, with the radii of the two populations on average ca. 50 and 300 nm [28].

2.4. Modification of QCM-D sensor chips

Absolute ethanol (≥99.7%), propan-2-ol (≥99.0%) and hydrogen peroxide (30%) were purchased from Merck (Kilsyth, Australia). Ammonium hydroxide solution (28%) was obtained from Ajax Finechem (Seven Hills, Australia). 3-Mercaptopropionic acid (MPA, ≥99.0%) was purchased from Fluka, BioChimica (Buchs, Switzerland). The QCM-D sensor crystals used were polished, gold-coated, AT-cut quartz chips with a fundamental frequency of ca. 5 MHz (Q-Sense, Västra Frölunda, Sweden). Immediately before measurements the chips were cleaned in a solution of ammonium hydroxide: hydrogen peroxide: water (1:1:3 v/v) for 20–25 min at ca. 70 °C. The chips were then rinsed thoroughly with water. Surface modification with MPA was conducted by immersing a freshly cleaned chip into a 1 mM solution of MPA in propan-2-ol for at least 1 h. This creates a self-assembled monolayer of negative charge on the chip surface. Excess MPA was removed by rinsing with propan-2-ol. The chips were then dried under N_2 and assembled into the QCM-D chambers ready for use.

2.5. QCM-D experiments

QCM-D experiments were performed using the E4 system with flow cells (Q-Sense, Västra Frölunda, Sweden). The QCM-D instrument measures the relative changes to the resonance frequency (f) and energy dissipation (D) of the chip over the course of the experiment. Δf and ΔD were measured simultaneously at the fundamental frequency and the 3rd, 5th, 7th and 9th harmonics. All plots presented in this study will use the 7th harmonic unless otherwise stated. Data for the fundamental frequency is not presented as it is inherently noisy and unreliable. The original data was processed in QTools (Q-Sense) before being exported for further analysis in OriginPro 8 (OriginLab Corp., Northampton, USA). All experiments were conducted at a temperature of 19.10 ± 0.05 °C and repeated at least three times.

In a typical experiment, firstly, a lipid membrane was formed on the chip surface by the introduction of a liposome solution into the QCM-D chamber at a flow rate of 50–100 μL/min. The liposomes adsorb onto the MPA-monolayer, deform, rupture and fuse together to form a lipid bilayer [28]. Weakly attached liposomes were removed by washing with high-salt PBS (100 mM NaCl) at 300 μL/min and any embedded liposomes were ruptured by washing with low-salt PBS (30 mM NaCl) at 300 μL/min. This second washing step was introduced to ensure the formation of a homogeneous membrane and works by creating an osmotic pressure difference between the interior of the embedded liposomes (having a high salt concentration) and the low-salt exterior environment, which causes the liposomes to swell and then burst. Secondly, after a stable baseline was observed, 1 mL of peptide solution (1, 2, 5, 10 and 15 μM in PBS) was introduced at 50 μL/min. After the flow was stopped, the peptide was left to incubate with the lipid membrane for 30 min and then the chamber was rinsed with high-salt PBS.

The change in mass of the chip (Δm) can be calculated using the Sauerbrey equation [29]:

$$\Delta m = -C\left(\frac{\Delta f n}{n}\right) \quad (1)$$

where C is the mass sensitivity constant (17.7 ng/cm^2·Hz for a chip with a fundamental frequency of 5 MHz) and n is the harmonic number. All mass values reported use the 7th harmonic ($n = 7$) unless otherwise stated. Cho and co-workers have demonstrated that the Sauerbrey equation effectively models lipid bilayers in aqueous buffer [30].

3. Results and discussion

3.1. QCM-D results for Tat interaction with mammalian membranes

The behaviour of Tat (44–57) and Tat (49–57) on mammalian-mimetic membranes is presented here as a comparison since, despite being the subject of intense debate, it is accepted that Tat does not disrupt mammalian cells (Tat penetration is thought to proceed via one or all of endocytosis, pore formation, inverted micelle formation and/or direct translocation [12,31,32]). A lipid combination of DMPC/cholesterol was used, as phosphocholine and cholesterol are the major constituents of mammalian membranes [33]. The model systems were kept as simple as possible to focus on the peptide–phospholipid interaction.

In a QCM-D instrument, an alternating-current (AC) voltage is applied across a quartz chip to cause the chip to oscillate in shear mode at its fundamental frequency (f_0) and harmonics of the fundamental frequency (f_n, where n is the harmonic number). The driving AC

voltage is periodically removed to measure the energy loss of the chip into the surrounding environment, giving the dissipation factor (D) [34]. The results from a typical QCM-D experiment are shown in Fig. 1. The Δf–time plot in panel A shows *changes in mass* over the course of the experiment; a decrease in Δf corresponds to an increase in mass density (see Equation (1) and ref. [29]). The ΔD–time plot in panel B shows *changes in structure*; an increase in ΔD means the chip dissipates its energy more quickly when the driving AC voltage is removed and suggests the film on the chip is thicker, softer or more loose [34,35]. The experiment in Fig. 1 commenced with the chip oscillating in high-salt PBS and at point (i) the liposome solution was introduced into the QCM-D chamber. This causes an increase in mass of the chip, as liposomes adsorb, deform, rupture and fuse to form a lipid membrane. Flow was stopped after a change in Δf of ca. −15 Hz, which corresponds to one complete bilayer (as explained in ref. [28]). A high-salt PBS rinse was performed at point (ii) to remove unadsorbed liposomes from the chamber. The decrease in mass resulting from the removal of weakly bound liposomes is offset by an increase in mass caused by residual liposomes from the tubing entering the QCM-D chamber and adsorbing and rupturing on the chip surface. At point (iii) the chamber was rinsed with low-salt PBS, which causes a rapid increase in Δf and decrease in ΔD. This is because of, firstly, the sensitivity of the resonance frequency and energy dissipation of the chip to the density and viscosity of the surrounding solution [36] and, secondly, the rupturing of embedded liposomes due to osmotic pressure difference. This rupturing expels water trapped inside the liposomes, causing the decrease in mass observed, and increases the rigidity of the membrane, resulting in the lower energy dissipation. The chamber was flushed with high-salt PBS at point (iv) until a baseline was established, whereupon the peptide solution was introduced at point (v). After allowing the peptide and membrane to incubate for 30 min, the chamber was washed with high-salt PBS at point (vi), concluding the experiment.

3.1.1. Tat (44–57) on DMPC/cholesterol

First we investigated the interaction of Tat with DMPC/cholesterol membranes over a concentration range of 1–15 μM, which corresponds to the MIC range for Tat on bacterial cells [11,18]. The results are presented in Fig. 2. On introduction of Tat (44–57) into the QCM-D chamber there was a small decrease in Δf, which corresponds to an increase in mass of the chip. This mass addition caused negligible change in ΔD ($<0.5 \times 10^{-6}$), suggesting that there is no change in the membrane structure. Similar results were observed for Tat (49–57) (data not shown).

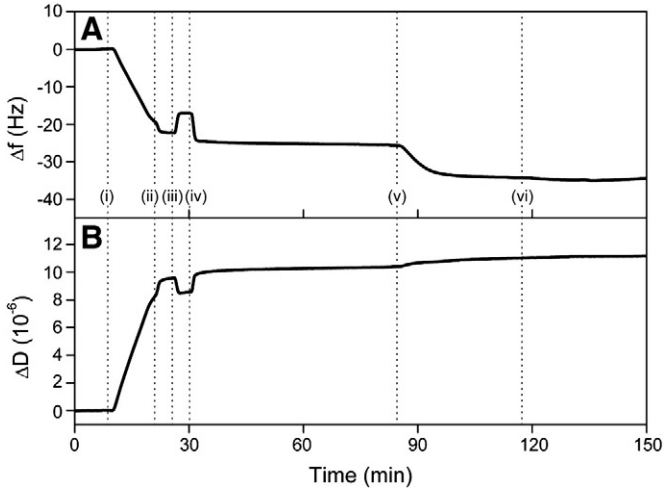

Fig. 1. Results for a typical QCM-D experiment. Δf–t (A) and ΔD–t (B) plots are presented. At time point (i) a liposome solution was introduced into the chamber; at points (ii), (iv) and (vi) the chamber was flushed with high-salt PBS; at point (iii) the chamber was flushed with low-salt PBS; and at point (v) the peptide solution was introduced into the chamber. See text for further explanation.

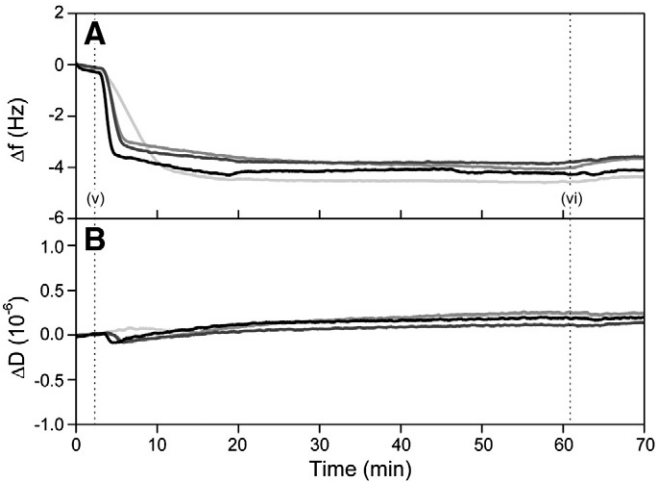

Fig. 2. Δf–t (A) and ΔD–t (B) plots obtained for the interaction of Tat (44–57) with a DMPC/cholesterol membrane. The response of four peptide concentrations is shown (1, 5, 10 and 15 μM; lightest to darkest lines). Time points (v) and (vi) correspond to peptide addition and buffer rinse, respectively.

Several conclusions can be drawn from Fig. 2. Firstly, as expected and consistent with the literature, Tat does not disrupt mammalian membranes; a one-step mass addition process was observed at all concentrations. Secondly, Tat addition only proceeds until membrane saturation is reached. That is, while the rate of Tat addition was dependent on the concentration of peptide in solution, the overall amount of peptide added was independent; a change in Δf of -4.0 ± 0.3 Hz ($\Delta m = 57 \pm 4$ ng) was observed for all concentrations. Thirdly, the buffer wash performed after incubation (point (vi) in Fig. 2) removes a negligible amount of material from the surface (<5%), which suggests that binding is irreversible. We have previously studied known membrane-penetrating AMPs e.g. apidaecin 1a and 1b and oncocin (peptide 10). They show a similar QCM-D response to Tat, i.e. peptide addition with no change in energy dissipation, however, on washing with buffer >50% of the bound peptide is removed [20,21,24]. Thus the strong affinity between Tat and the membrane is unique compared with some other cell-penetrating peptides that we have studied using QCM-D.

These conclusions are consistent with three possible mechanisms. The first mechanism involves strong Tat binding to the phosphate residues of the membrane. Shaw and co-workers observed using atomic force microscopy that bilayer association of Tat was phase-dependent, causing an apparent height increase of liquid-phase domains (either due to peptide aggregation on or membrane restructuring of these domains) [37]. At the cholesterol concentration of 30 mol% used in our experiments only the liquid-ordered phase would be present [38,39]. Thus the small increase in ΔD upon peptide addition could be explained by the height increase observed by Shaw et al. However, according to Shaw et al. there should be a difference between Tat interaction with gel-phase DMPC and liquid-ordered phase DMPC/cholesterol membranes. We observed negligible difference between the two membranes (data not shown), suggesting either that Tat association is not always phase-dependent or our experimental conditions are promoting a different mechanism of action. Furthermore, Dennison and co-workers demonstrated that Tat (48–60) binds weakly to DMPC monolayers, due to its low hydrophobicity [40]. This first mechanism would therefore be unlikely according to their study, as we observed an irreversible and strong association to the membrane.

Secondly, and alternatively, the QCM-D data is consistent with pore formation, which has been observed experimentally and demonstrated in silico [41–45]. We have previously postulated that if the change in resonance frequency is similar for all harmonics in an experiment, this is an indication that the peptide has inserted into the membrane in a transmembrane manner [22]. This is because the depth probed by a harmonic is inversely proportional to its frequency [46]; higher harmonics probe close to the surface of the chip and lower harmonics probe further away from the surface. If all harmonics measure the same change in frequency, this means that mass density is the same across the whole thickness of the membrane (i.e. pore formation). This is observed for Tat addition to DMPC/cholesterol (data not shown).

The third mechanism is direct translocation through the membrane. Tat penetration has been observed in the absence of endocytosis or pore formation, hinting to the existence of a currently unspecified direct translocation mechanism [31,47]. In our experiments the membrane is supported by a negatively charged carboxylic acid-terminated monolayer. It is possible that the highly positively charged Tat penetrates through the membrane and binds to this MPA-monolayer. This would weaken the interaction between the sensor chip and the membrane, resulting in the increase in energy dissipation observed.

Therefore, the QCM-D results are consistent with three alternative mechanisms that cannot be distinguished using this data alone. We are currently employing complementary techniques to further clarify the mechanism of action. However, the interaction of Tat with DMPC/cholesterol provides an experiment from which we can compare the behaviour of Tat on bacterial-mimetic membranes.

3.2. QCM results for Tat interaction with bacterial membranes

3.2.1. Tat (49–57) on DMPC/DMPG 4:1

A DMPC/DMPG (4:1) membrane is used as the model system for prokaryotic membranes, as the inclusion of DMPG mimics the negatively charged components found on the surface of bacteria [48]. The behaviour of Tat (49–57) on this membrane is shown in Fig. 3. It is important to point out that Fig. 3 presents one peptide concentration and the response of four different harmonics (cf. Fig. 2). The results show that interaction between Tat (49–57) and DMPC/DMPG (4:1) occurs via a biphasic mechanism: peptide addition followed by membrane disruption. On introduction of the peptide into the QCM-D chamber, there was a decrease in frequency of ca. 4 Hz at all harmonics. This value was consistent across all experiments ($\Delta f_{av} = -3.8 \pm 0.7$ Hz). After membrane saturation was reached, mass was removed from the chip surface in a harmonic-dependent manner. That is, the greatest mass loss was observed at the 3rd and 5th harmonics, which probe further from the chip surface, while less mass loss was observed at the chip surface-sensing 7th and 9th harmonics (Fig. 3A). Therefore, disruption occurs on the surface of the membrane; consistent with a "carpet mechanism" [19,22,24]. The loss of mass was accompanied by a decrease in ΔD (Fig. 3B). This is because energy dissipation is proportional to thickness, according to the Kelvin–Voigt model of viscoelasticity. Furthermore, highly dissipating bilayer patches sitting on top of the complete bilayer may have been removed, contributing to the decrease in ΔD. The buffer rinse performed at the end of the experiment (point (vi) in Fig. 3) resulted in a negligible change in mass.

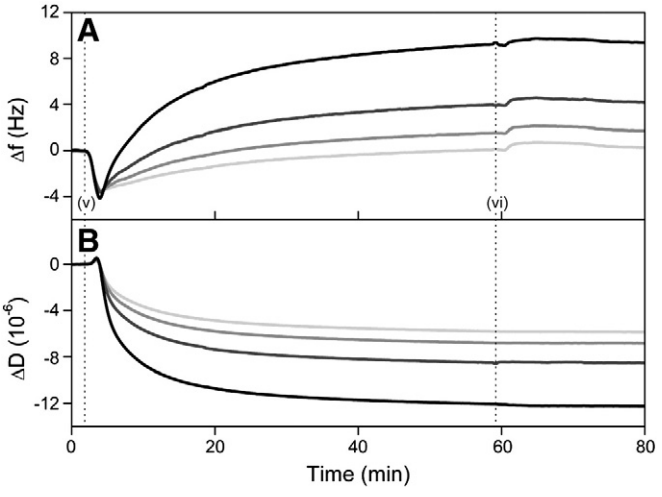

Fig. 3. Δf–t (A) and ΔD–t (B) plots obtained for the interaction of a 10 μM solution of Tat (49–57) with a DMPC/DMPG 4:1 membrane. The response of four harmonics is shown (3rd, 5th, 7th and 9th harmonics; darkest to lightest lines). Time points (v) and (vi) correspond to peptide addition and buffer rinse, respectively.

Disruption of PC/PG membranes has not been previously observed. Thorén and co-workers reported that TatP59W (Ac-GRKKRRQRRRPWQ-NH_2) caused the leakage of only 1.9% of entrapped carboxyfluorescein from DOPC/DOPG (3:2) vesicles [17]. Zhu and Shin reported that Tat (48–60; GRKKRRQRRRPPQ) induced the release of ca. 10% of entrapped calcein from egg yolk phosphoethanolamine/PG (7:3) vesicles [18]. Under the same conditions, TatP59W caused the leakage of ca. 20% of the fluorescent dye [18], in contrast to the 1.9% determined by Thorén et al. Ruzza and co-workers observed that Tat (48–61; GRKKRRQRRRPPQG) caused the leakage of ca. 10% of calcein from DMPC/DMPG (3:1) vesicles [15]. Finally, Yang and co-workers reported that Tat (48–61; GRKKRRQRRRPPQC) caused <5% leakage of ANTS/DPX dye from DOPC/DOPG (1:1) vesicles [49]. Therefore, experimental differences could explain the discrepancy between the results of this study and earlier work. Firstly, higher peptide concentrations were used in our study (1–15 μM) and significant loss of mass from the membrane was only observed at concentrations above 5 μM. This concentration range is lower than the MIC values of Tat of 0.6–20 μM as determined by Jung et al. [11]. Secondly, Tat (44–57) and Tat (49–57) peptides were studied here and differences in sequence will change membrane activity (see below). Thirdly, the aforementioned studies were conducted on bilayers in the liquid-phase, whereas in our study the bilayers were in the gel-phase. Membrane defects tend to exist in bilayers formed below their phase-transition temperature and it is possible that these defects make the membrane more susceptible to disruption [50]. Finally, the dye-leakage studies summarised above used small (≤100 nm) vesicles, which exhibit high shear moduli, lower deformation, and hence are less likely to undergo disruption compared with planar bilayers [28,51]. The results of this study are, therefore, not inconsistent with the existing literature but instead outline a set of prerequisite factors for observable bacterial membrane disruption by the Tat peptide.

3.2.2. Effect of hydrophobicity of Tat and negative charge of membrane

The effect of peptide hydrophobicity on bacterial membrane disruption was investigated by using the longer-sequence peptide Tat (44–57). Both Tat (49–57) and Tat (44–57) have a net charge of +9 at pH 7.4. However, the free energy of transfer from water to lipid interface for Tat (44–57) is 3.77 kcal/mol and for Tat (49–57) it is 4.87 kcal/mol, according to the Wimley and White (WW) scale [52,53]. That is, Tat (44–57) is more hydrophobic than Tat (49–57). The effect of membrane charge was investigated by increasing the percentage of DMPG in the membrane from 20% to 33%. The results are presented as plots of Δf versus ΔD in Fig. 4 (called "Δf–ΔD plots"). A comprehensive explanation of the interpretation of Δf–ΔD plots can be found in ref. [24]. In summary, these plots illustrate how the structure of the lipid membrane changes per unit mass addition [35]. Each discrete point in the plot represents the value of Δf and ΔD at a certain time. In Fig. 4, the point (0,0) corresponds to the time when the peptide solution was introduced into the QCM-D chamber. The last point in each trace corresponds to the end of the incubation

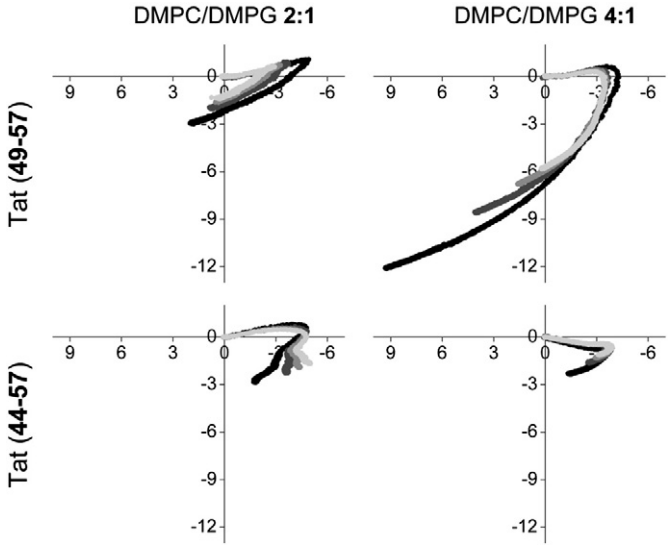

Fig. 4. Representative Δf–ΔD plots for the interaction of a 10 μM solution of either Tat (49–57) or Tat (44–57) on a DMPC/DMPG 2:1 or 4:1 membrane. The *x*-axis is Δf and the *y*-axis is ΔD. The coordinate (0,0) corresponds to the time when the peptide solution was introduced into the QCM-D chamber. Time increases along the trace and the last point in the trace corresponds to the end of the incubation period (i.e. the time window from points (v) to (vi) is shown; see Fig. 1). The response of the 3rd, 5th, 7th and 9th harmonics is presented (darkest to lightest dots).

period. That is, the time window from points (v) to (vi) is presented (see Fig. 1).

For example, for Tat (49–57) on DMPC/DMPG 4:1 in Fig. 4 (top-right panel) the Δf–ΔD plot has one turning point at $\Delta f \approx -3$ Hz and $\Delta D \approx 0$. Therefore, it interacts with the membrane via a two-phase mechanism [24]. The first phase can be described by an arrow beginning at (0,0) and ending at the turning point at (−3,0). Using Fig. 5 as a guide, it can be seen that this due east arrow corresponds to mass addition with no change in membrane structure. The second phase can be described by an arrow beginning at the turning point at (−3,0) and ending at the last point in the trace (e.g. point (0,−6) for the 9th harmonic). This is a south-west arrow, which corresponds to mass loss and increase in rigidity of the membrane. This south-west arrow extends into $+\Delta f$ values, which indicates a net loss of mass from the surface and not merely a desorption of peptide. Therefore, either using the Δf–*t* and ΔD–*t* plots or one Δf–ΔD plot, the same conclusion that Tat interacts with bacterial membranes according to a biphasic mechanism is reached. Δf–ΔD plots are used in this section of the article because they enable easy comparison between different QCM-D experiments (see Fig. 4).

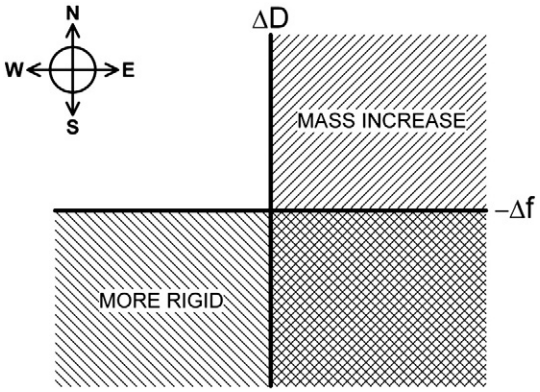

Fig. 5. Interpretative guide for Δf–ΔD plots. This guide was first introduced by us in ref. [24] to assist in the interpretation of Δf–ΔD plots.

For both Tat peptides, less membrane disruption was observed on the more negatively charged DMPC/DMPG (2:1) membranes (Fig. 4). This seems counter-intuitive; prima facie, more peptide would be expected to bind to the more negatively charged membrane in order to achieve charge neutralisation, inducing greater stress in the membrane and causing larger disruption. Indeed, more peptide was observed to bind to the DMPC/DMPG (2:1) membranes (e.g. for Tat (49–57), $\Delta f_{av} = -5.8 \pm 1.3$ for 2:1 membrane versus $\Delta f_{av} = -3.7 \pm 1.3$ for 4:1 membrane, at the 3rd harmonic). Thus increasing the negative charge on the membrane increases the amount of Tat that adsorbs. However, this increased adsorption does not lead to increased disruption. The reason for reduced disruption on DMPC/DMPG (2:1) must be due to how the Tat peptides interact with the surface. It was demonstrated by Ruzza and co-workers that Tat (48–61) shows a lower affinity towards neat DMPG liposomes than DMPC/DMPG (3:1) liposomes [15]. Similarly, various oligoarginines (R_6, R_8 and R_{10}) all exhibited lower affinity towards the more negatively charged DMPG liposomes [15]. This suggests that both electrostatic and hydrophobic interactions dictate binding strength [15,54]. Increasing the negative charge of the membrane may increase electrostatic attraction, but binding strength is lowered overall because of weakened hydrophobic interactions. Lower affinity means less stress is placed on the membrane and, therefore, less disruption is observed on DMPC/DMPG (2:1) membranes compared with DMPC/DMPG (4:1) membranes.

On both membranes, less disruption was observed for the more hydrophobic Tat (44–57) peptide (Fig. 4). This result seems inconsistent with the analysis above. Indeed, Zhu and Shin reported that the more hydrophobic TatP59W had smaller MIC values and induced more dye leakage in bacterial-mimetic liposomes than the native Tat peptide [18]. Furthermore, Thorén and co-workers hypothesised that this tryptophan substitution would reorientate the amidated C-terminus of the peptide deeper into the membrane, creating defects in lipid packing that should enhance membrane destabilisation [17]. However, in Tat (44–57) the hydrophobic residues Ile45 and Tyr47 are separated by hydrophilic Ser46 and are located near the hydrophilic acetylated N-terminus. Therefore, it is unlikely that the N-terminus would protrude into the membrane interior as Thorén et al. suggested for their peptides. Similarly, Zhu and Shin were comparing Tat (48–60), with a WW free energy of 8.64 kcal/mol, with amidated TatP59W, which has a WW free energy of 4.44 kcal/mol. Therefore, the difference in liposome dye leakage between the two peptides is explained by the drastic difference in hydrophobicity (95% variation in free energy values). In our study, this difference is much less (30%). Because the difference in hydrophobicity between Tat (44–47) and Tat (49–57) is relatively small it is possible that other differences between the two peptides dominate. For example, length may be a determining factor. The shorter Tat (49–57) peptide may enable closer packing, resulting in a greater membrane strain over a smaller area, which would enhance membrane disruption. Several groups have reported that increasing peptide length increases antimicrobial activity [55,56]. However, these studies investigated the effect of length by varying the number of repeat units e.g. $(RW)_n$-NH_2 (where $n = 1$–5) [56]. This means the interaction between peptide and membrane will be consistent over the length of the peptide. In our study, the longer Tat (44–57) is not necessary more active, because the $^{44}GISYG_{48}$ unit may have no activity. Therefore, the slight increase in hydrophobicity, the inability of the N-terminus to protrude into the membrane and the longer length of Tat (44–57) may explain why it exhibits less disruptive activity compared with Tat (49–57).

4. Conclusion

In this study, we determined that two truncated Tat sequences, Tat (44–57) and Tat (49–57), exert their antimicrobial activity via the

carpet-like mechanism on planar, gel-phase DMPC/DMPG lipid membranes. This surface-active mechanism occurs in two stages, both observable in the QCM-D data. Firstly, the Tat peptides bind to the membrane surface. The adsorption amount is proportional to the negative charge of the membrane; the higher the negative charge, the greater the amount of peptide that adsorbs to achieve charge neutralisation. Secondly, after a threshold surface coverage is reached, the peptides disintegrate the membrane by disrupting the membrane structure [3]. Both electrostatic and hydrophobic interactions determine the peptide-lipid binding strength and, thus, the magnitude of membrane disruption. For example, even though more peptide adsorbed onto the more negatively charged DMPC/DMPG (2:1) membranes, less disruption was observed due to weakened hydrophobic interactions. Furthermore, the length of the peptide may be important. It was observed that Tat (44–57) was less active than the shorter Tat (49–57). The shorter peptide may induce a greater membrane strain per unit area, increasing disruption. Finally, as a comparison it was determined that neither Tat sequence disrupted the mammalian-mimetic DMPC/cholesterol membranes, consistent with the reports that Tat exerts no hemolytic activity [10,11,18]. Our results suggest that Tat does not simply act through an intracellular mechanism but also acts on the bacterial membrane, making it a promising antibiotic for further development [7].

Acknowledgements

Financial support from grants from the Australian Research Council (ARC) and National Health and Medical Research Council (NH&MRC) to L.L.M. is acknowledged.

References

[1] IDSA, bad bugs, no drugs: as antibiotic discovery stagnates, a public health crisis brews (2004). http://www.idsociety.org/. Accessed 28 Sept 2010.
[2] M.L. Katz, L.V. Mueller, M. Polyakov, S.F. Weinstock, Where have all the antibiotic patents gone? Nat. Biotechnol. 24 (2006) 1529–1531.
[3] Y. Shai, Mode of action of membrane active antimicrobial peptides, Biopolymers 66 (2002) 236–248.
[4] D.W. Hoskin, A. Ramamoorthy, Studies on anticancer activities of antimicrobial peptides, Biochim. Biophys. Acta 1778 (2008) 357–375.
[5] G. Wang, X. Li, Z. Wang, APD2: the updated antimicrobial peptide database and its application in peptide design, Nucleic Acids Res. 37 (2009) D933–D937.
[6] M. Zasloff, Antimicrobial peptides of multicellular organisms, Nature 415 (2002) 389–395.
[7] A. Peschel, H.-G. Sahl, The co-evolution of host cationic antimicrobial peptides and microbial resistance, Nat. Microbiol. 4 (2006) 529–536.
[8] R. Pálffy, R. Gardlík, M. Behuliak, L. Kadasi, J. Turna, P. Celec, On the physiology and pathophysiology of antimicrobial peptides, Mol. Med. 15 (2009) 51–59.
[9] L.M. Gottler, A. Ramamoorthy, Structure, membrane orientation, mechanism, and function of pexiganan—a highly potent antimicrobial peptide designed from magainin, Biochim. Biophys. Acta 1788 (2009) 1680–1686.
[10] H.J. Jung, Y. Park, K.-S. Hahm, D.G. Lee, Biological activity of Tat (47–58) peptide on human pathogenic fungi, Biochem. Biophys. Res. Commun. 345 (2006) 222–228.
[11] H.J. Jung, K.-S. Jeong, D.G. Lee, Effective antibacterial action of Tat (47–58) by increased uptake into bacterial cells in the presence of trypsin, J. Microbiol. Biotechnol. 18 (2008) 990–996.
[12] I. Green, R. Christison, C.J. Voyce, K.R. Bundell, M.A. Lindsay, Protein transduction domains: are they delivering? Trends Pharmacol. Sci. 24 (2003) 213–215.
[13] R. Tréhin, H.P. Merkle, Chances and pitfalls of cell penetrating peptides for cellular drug delivery, Eur. J. Pharm. Biopharm. 58 (2004) 209–223.
[14] H. Brooks, B. Lebleu, E. Vivès, Tat peptide-mediated cellular delivery: back to basics, Adv. Drug Deliv. Rev. 57 (2005) 559–577.
[15] P. Ruzza, B. Biondi, A. Marchiani, N. Antolini, A. Calderan, Cell-penetrating peptides: a comparative study on lipid affinity and cargo delivery properties, Pharmaceuticals 3 (2010) 1045–1062.
[16] E. Eiríksdóttir, K. Konate, Ü. Langel, G. Divita, S. Deshayes, Secondary structure of cell-penetrating peptides controls membrane interaction and insertion, Biochim. Biophys. Acta 1798 (2010) 1119–1128.
[17] P.E.G. Thorén, D. Persson, P. Lincoln, B. Nordén, Membrane destabilizing properties of cell-penetrating peptides, Biophys. Chem. 114 (2005) 169–179.
[18] W.L. Zhu, S.Y. Shin, Effects of dimerization of the cell-penetrating peptide Tat analog on antimicrobial activity and mechanism of bactericidal action, J. Pept. Sci. 15 (2009) 345–352.
[19] Y. Shai, Mechanism of the binding, insertion and destabilization of phospholipid bilayer membranes by α-helical antimicrobial and cell non-selective membrane-lytic peptides, Biochim. Biophys. Acta 1462 (1999) 55–70.
[20] S. Piantavigna, P. Czihal, A. Mechler, M. Richter, R. Hoffmann, L.L. Martin, Cell penetrating apidaecin peptide interactions with biomimetic phospholipid membranes, Int. J. Pept. Res. Ther. 15 (2009) 139–146.
[21] D. Knappe, S. Piantavigna, A. Hansen, A. Mechler, A. Binas, O. Nolte, L.L. Martin, R. Hoffmann, Oncocin (VDKPPYLPRPRPPRRIYNR-NH2): a novel antibacterial peptide optimized against Gram-negative human pathogens, J. Med. Chem. 53 (2010) 5240–5247.
[22] A. Mechler, S. Praporski, K. Atmuri, M. Boland, F. Separovic, L.L. Martin, Specific and selective peptide-membrane interactions revealed using quartz crystal microbalance, Biophys. J. 93 (2007) 3907–3916.
[23] P.J. Sherman, R.J. Jackway, J.D. Gehman, S. Praporski, G.A. McCubbin, A. Mechler, L.L. Martin, F. Separovic, J.H. Bowie, Solution structure and membrane interactions of the antimicrobial peptide fallaxidin 4.1a: an NMR and QCM study, Biochemistry 48 (2009) 11892–11901.
[24] G.A. McCubbin, S. Praporski, S. Piantavigna, D. Knappe, R. Hoffmann, J.H. Bowie, F. Separovic, L.L. Martin, QCM-D fingerprinting of membrane-active peptides, Eur. Biophys. J. 40 (2011) 437–446.
[25] K. Christ, I. Wiedemann, U. Bakowsky, H.-G. Sahl, G. Bendas, The role of lipid II in membrane binding of and pore formation by nisin analyzed by two combined biosensor techniques, Biochim. Biophys. Acta 1768 (2007) 694–704.
[26] S.B. Nielsen, D.E. Otzen, Impact of the antimicrobial peptide Novicidin on membrane structure and integrity, J. Colloid Interface Sci. 345 (2010) 248–256.
[27] C.A. Keller, B. Kasemo, Surface specific kinetics of lipid vesicle adsorption measured with a quartz crystal microbalance, Biophys. J. 75 (1998) 1397–1402.
[28] A. Mechler, S. Praporski, S. Piantavigna, S.M. Heaton, K.N. Hall, M.-I. Aguilar, L.L. Martin, Structure and homogeneity of pseudo-physiological phospholipid bilayers and their deposition characteristics on carboxylic acid terminated self-assembled monolayers, Biomaterials 30 (2009) 682–689.
[29] G. Sauerbrey, The use of quartz oscillators for weighing thin layers and for microweighing, Z. Phys. 155 (1959) 206–222.
[30] N.-J. Cho, K.K. Kanazawa, J.S. Glenn, C.W. Frank, Employing two different quartz crystal microbalance models to study changes in viscoelastic behavior upon transformation of lipid vesicles to a bilayer on a gold surface, Anal. Chem. 79 (2007) 7027–7035.
[31] S.T. Henriques, M.N. Melo, M.A.R.B. Castanho, Cell-penetrating peptides and antimicrobial peptides: how different are they? Biochem. J. 399 (2006) 1–7.
[32] N. Schmidt, A. Mishra, G.H. Lai, G.C.L. Wong, Arginine-rich cell-penetrating peptides, FEBS Lett. 584 (2010) 1806–1813.
[33] G. van Meer, D.R. Voelker, G.W. Feigenson, Membrane lipids: where they are and how they behave, Nat. Rev. Mol. Cell Biol. 9 (2008) 112–124.
[34] M. Rodahl, F. Höök, A. Krozer, P. Brzezinski, B. Kasemo, Quartz crystal microbalance setup for frequency and Q-factor measurements in gaseous and liquid environments, Rev. Sci. Instrum. 66 (1995) 3924–3930.
[35] M. Rodahl, F. Höök, C. Fredriksson, C.A. Keller, A. Krozer, P. Brzezinski, M. Voinova, B. Kasemo, Simultaneous frequency and dissipation factor QCM measurements of biomolecular adsorption and cell adhesion, Faraday Discuss. 107 (1997) 229–246.
[36] K.K. Kanazawa, J.G. Gordon, Frequency of a quartz microbalance in contact with liquid, Anal. Chem. 57 (1985) 1770–1771.
[37] J.E. Shaw, R.F. Epand, J.C.Y. Hsu, G.C.H. Mo, R.M. Epand, C.M. Yip, Cationic peptide-induced remodelling of model membranes: direct visualization by in situ atomic force microscopy, J. Struct. Biol. 162 (2008) 121–138.
[38] H.J. Hinz, J.M. Sturtevant, Calorimetric investigation of the influence of cholesterol on the transition properties of biolayers formed from synthetic L-α-lecithins in aqueous suspension, J. Biol. Chem. 247 (1972) 3697–3700.
[39] S.L. Veatch, S.L. Keller, Seeing spots: complex phase behavior in simple membranes, Biochim. Biophys. Acta 1746 (2005) 172–185.
[40] S.R. Dennison, R.D. Baker, I.D. Nicholl, D.A. Phoenix, Interactions of cell penetrating peptide Tat with model membranes: a biophysical study, Biochem. Biophys. Res. Commun. 363 (2007) 178–182.
[41] A. Mishra, V.D. Gordon, L. Yang, R. Coridan, G.C.L. Wong, HIV TAT forms pores in membranes by inducing saddle-splay curvature: potential role of bidentate hydrogen bonding, Angew. Chem. Int. Ed. 47 (2008) 2986–2989.
[42] C. Ciobanasu, J.P. Siebrasse, U. Kubitscheck, Cell-penetrating HIV1 TAT peptides can generate pores in model membranes, Biophys. J. 99 (2010) 153–162.
[43] H.D. Herce, A.E. Garcia, Molecular dynamics simulations suggest a mechanism for translocation of the HIV-1 TAT peptide across lipid membranes, PNAS 104 (2007) 20805–20810.
[44] S. Yesylevskyy, S.-J. Marrink, A.E. Mark, Alternative mechanisms for the interaction of the cell-penetrating peptides penetratin and the TAT peptide with lipid bilayers, Biophys. J. 97 (2009) 40–49.
[45] H.D. Herce, A.E. Garcia, J. Litt, R.S. Kane, P. Martin, N. Enrique, A. Rebolledo, V. Milesi, Arginine-rich peptides destabilize the plasma membrane, consistent with a pore formation translocation mechanism of cell-penetrating peptides, Biophys. J. 97 (2009) 1917–1925.
[46] M. Rodahl, B. Kasemo, On the measurement of thin liquid overlayers with the quartz-crystal microbalance, Sens. Actuators A 54 (1996) 448–456.
[47] G. Ter-Avetisyan, G. Tünnemann, D. Nowak, M. Nitschke, A. Herrmann, M. Drab, M.C. Cardoso, Cell entry of arginine-rich peptides is independent of endocytosis, J. Biol. Chem. 284 (2009) 3370–3378.

[48] C.S.B. Chia, J. Torres, M.A. Cooper, I.T. Arkin, J.H. Bowie, The orientation of the antibiotic peptide maculatin 1.1 in DMPG and DMPC lipid bilayers. Support for a pore-forming mechanism, FEBS Lett. 512 (2002) 47–51.
[49] S.-T. Yang, E. Zaitseva, L.V. Chernomordik, K. Melikov, Cell-penetrating peptide induces leaky fusion of liposomes containing late endosome-specific anionic lipid, Biophys. J. 99 (2010) 2525–2533.
[50] L. Bakás, H. Ostolaza, W.L.C. Vaz, F.M. Goñi, Reversible adsorption and nonreversible insertion of *Escherichia coli* α-hemolysin into lipid bilayers, Biophys. J. 71 (1996) 1869–1876.
[51] P.E.G. Thorén, D. Persson, E.K. Esbjörner, M. Goksör, P. Lincoln, B. Nordén, Membrane binding and translocation of cell-penetrating peptides, Biochemistry 43 (2004) 3471–3489.
[52] W.C. Wimley, S.H. White, Experimentally determined hydrophobicity scale for proteins at membrane interfaces, Nat. Struct. Biol. 3 (1996) 842–848.
[53] C. Snider, S. Jayasinghe, K. Hristova, S.H. White, MPEx: a tool for exploring membrane proteins, Protein Sci. 18 (2009) 2624–2628.
[54] L.-P. Liu, C.M. Deber, Anionic phospholipids modulate peptide insertion into membranes, Biochemistry 36 (1997) 5476–5482.
[55] L. Ringstad, A. Schmidtchen, M. Malmsten, Effect of peptide length on the interaction between consensus peptides and DOPC/DOPA bilayers, Langmuir 22 (2006) 5042–5050.
[56] Z. Liu, A. Brady, A. Young, B. Rasimick, K. Chen, C. Zhou, N.R. Kallenbach, Length effects in antimicrobial peptides of the $(RW)_n$ series, Antimicrob. Agents Chemother. 51 (2007) 597–603.